VNU Journal of Science: Mathematics – Physics, Vol. 40, No. 1 (2024) 95-104

VNU Journal of Science: Mathematics - Physics

Journal homepage: https://js.vnu.edu.vn/MaP

Original Article

Clarifying Contribution of SERS Mechanism Based on Semiconductor Material - ZnO Microtube in Probing Methylene Blue

Tran Thu Trang*

Institute of Sciences and Technology, TNU University of Sciences, Tan Thinh, Thai Nguyen, Vietnam

Received 06 November 2023
Revised 27 November 2023; Accepted 18 March 2024

Abstract: Surface-enhanced Raman spectroscopy (SERS) is a powerful technique for identifying molecular species, but it has been primarily limited to noble metal supports. The use of semiconductor materials as SERS surfaces has been attempted and has generally proven less effective than metal materials. It is known due to semiconductor materials' less efficient surface plasmon resonance (SPR) effect mechanism. This study clarified the SERS mechanism based on semiconductor material - ZnO microtube in probing methylene blue (MB) as an equal contribution of charge transfer and SPR mechanisms. Using Herzberg-Teller-surface selection rules, the charge transfer contribution in the SERS mechanism was estimated at approximately 50%. The limit of detection of ZnO microtube was achieved at 10^{-7} M, and the best enhancement factor was of 6.1×10^{5}.

Keywords: SERS mechanisms, charge transfer contribution, ZnO microtube.

1. Introduction

Surface-enhanced Raman scattering (SERS) spectroscopy, which uses abundant fingerprint information, is a powerful technique for the highly sensitive, rapid, and non-destructive detection of trace various chemical molecules [1]. The enhancement mechanism has been proposed mostly from surface plasmon resonance (SPR) contribution, which provides a major contribution; chemical mechanism enhancement is a minor contribution [2]. According to the calculations, the maximum enhancement factor (EF) originating from the electromagnetic mechanism can reach 10^{11} orders of magnitude [3]. Meanwhile, the chemical mechanism only makes a minor contribution, which is

* Corresponding author.
E-mail address: trangtt@tnus.edu.vn

https//doi.org/10.25073/2588-1124/vnumap.4888

generally explained by the charge transfer mechanism [4]. As a result, the theoretical calculation indicated that the EF could reach 10^4, much less than that in comparison to the SPR mechanism. It is well-known that noble metals have been shown as conventional materials for SERS applications at which SPR (due to the existence of free electrons) plays a pivotal role in Raman enhancements [5]. In semiconductors, the chemical mechanism enhancement generally acts as a predominant part that results from completely or partially bound electrons [6]. Although noble metal materials possess good properties for SERS application, their cost, poor stability and biocompatibility are the main disadvantages to widening this class of materials [7, 8].

Semiconductor materials have been paid much attention due to various interesting optical, chemical, and catalytic properties. Raman enhancement has been demonstrated in a few semiconducting materials, such as InAs/GaAs quantum dots [9], CuTe nanocrystals [10], and TiO_2 nanostructures [11], in which charge transfer at the semiconductor-analyte interface plays a significant role in Raman scattering enhancement. Charge transfer mechanism was also pointed as a primary cause of SERS activity of the ZnO microplate [12]. Because of its properties and functionality, ZnO has been identified as a promising candidate for SERS operation. In particular, ZnO is an n-type semiconductor and piezoelectric material with a large and tuneable band-gap energy (3.37 eV), a high exciton binding energy (60 meV), biocompatibility, ease of fabrication, and low cost of synthesis.

The SPR mechanism based on semiconductor material surfaces is generally less efficient than that of noble metal surfaces. Conversely, the charge transfer mechanism is typically more critical in semiconductor substrates. Using semiconductor surfaces to study charge transfer mechanisms is thus an appropriate strategy. Methylene blue (MB) is a cationic dye that is commonly used in industry and household products. It is widely used as a powerful drug to treat ischemia, septic shock, and a variety of other diseases [13]. MB belongs to the C_2 group symmetry and has 38 atoms and 108 fundamental modes of vibrations, in which 54 normal modes represent totally symmetric vibrations (A) and 54 vibration modes are non-symmetric modes [13]. Study of the SERS mechanism of MB molecules based on Cu/Cu_2O core/cell substrate revealed that the charge transfer mechanism contributed to SERS activity by about 36% [7].

In this work, ZnO microtube material was prepared by the hydrothermal route and then used as a SERS substrate to detect MB. The contribution of each mechanism has deciphered the SERS mechanism based on ZnO microtube surface. Using Herzberg-Teller-surface selection rules, the SPR and charge-transfer mechanism on ZnO microtube SERS surface revealed an equal contribution. The limit of detection (LOD) of MB using ZnO microtube substrate is as low as 10^{-7} M with the largest enhancement factor (EF) archives of 6.1×10^5.

2. Experiment Section

2.1. Materials

Zinc acetate ($Zn(OCOCH_3)_2$ 99,9% – $Zn(OAc)_2$), Zinc nitrate hexahydrate $Zn(NO_3)_2.6H_2O$, ammonia solution NH_4OH (25%), and absolute ethanol (C_2H_5OH, purity 99.7%) were purchased from Merck firm (Germany). All chemicals were used exactly as supplied, with no changes. Deionized water was used in all of the experiments, from cleaning glassware to making the solutions.

2.2. Synthesis of ZnO Microtubes

The hydrothermal processes were used to fabricate ZnO microtubes [14]. In a typical experiment, 13 ml 0.2 M NH_4OH solution was added dropwise into the prepared 100 ml $Zn(NO_3)_2$ (0.5 M) solution

in a beaker. After that, the mixture solution was stirred for 30 minutes using a magnetic stirrer at room temperature. Next, the obtained solution was heated to 180 ^{o}C in a Teflon-lined stainless autoclave and kept there for 40 hours.

The reaction equation of the above processes is as follows:

$$Zn(NO_3)_2+6NH_4OH \rightarrow Zn(NH_3)_4(OH)_2+2NH_4NO_3+4H_2O \quad (1)$$

$$Zn(NH_3)_4(OH)_2 \rightarrow ZnO+4NH_3+H_2O \quad (2)$$

After naturally cooling to room temperature, the white precipitate was harvested and rinsed several times with distilled water and absolute ethanol before being dried in the air at 80 ^{o}C overnight.

2.3. Characterization

The morphology of the microstructure under preparation was investigated using a 10 kV Hitachi S4800 scanning electron microscope (SEM). The interaction between electron beams and the surface of the sample provides surface topography information. Then, the SEM technique is able to directly measure the size and evaluate the shape of the sample. X-ray diffraction spectra were obtained using Cu K (0.154056 nm) radiation on an X-ray diffractometer (Bruker D8 Advance, Germany). A Raman spectrometer (Raman Horiba Zplora plus Raman microprobe, France) was used to record the normal Raman and SERS spectra of MB. Raman spectra were collected using laser excitation at 532 nm with a power of 3.2 mW and an acquisition time of 8 seconds for each measurement. The spectrometer was calibrated using a silicon wafer with a characteristic band of 520 cm^{-1}. SERS studies based on ZnO microtube were implemented to probe MB on the concentration range of 10^{-3} to 10^{-7} M. For SERS surface preparation, 30 µl of MB solution was dropped onto each surface for each concentration.

3. Results and Discussion

3.1. Structure Characterization

Firstly, the size and shape of the fabricated sample were examined using a scanning electron microscope (SEM) image. The sample indicated a highly uniform microtube morphology with an average length and diameter of about 3 µm and 0.3 µm, respectively (Fig. 1).

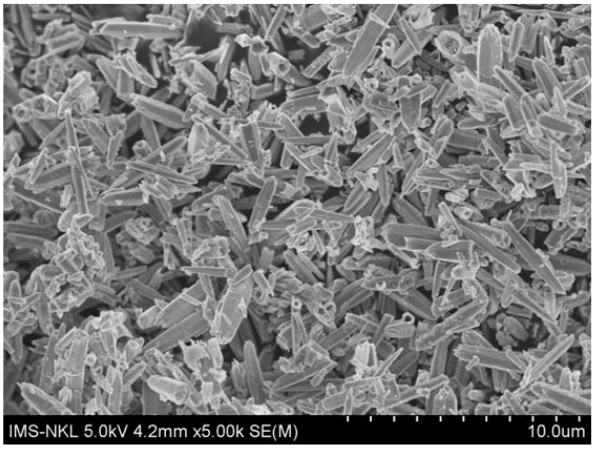

Figure 1. SEM image of ZnO microtube.

To account for the structure of the ZnO microtube, the X-Ray diffraction (XRD) pattern and Raman spectroscopy of the ZnO microtube were measured and presented in Fig. 2. All the XRD diffraction peaks of the ZnO microtube in Fig. 2a can be attributed to the ZnO wurtzite structure (JCPDS, 36-1451 card mo: 36-1451) [15]. Most XRD peaks are clearly intense and devoid of any impurity phases. This demonstrates that the ZnO was well crystallized. Futhermore, Raman vibration modes of the ZnO microtube also describe well properties of the ZnO structure (Fig. 2b). In more details, an intense peak at 439 cm^{-1} noted as E_2^{high} corresponds to the vibrations of the oxygen atoms. vimode of wurtzite ZnO structure. Some other peaks of the wurtzite ZnO structure are also detected at 331 cm^{-1} (named $2E_2^{low}$); 380 cm^{-1} (noted as A_1(TO)); and the vibrational modes at around 570 cm^{-1}, commonly known as the mixture of two modes A1 (LO) and E1 (LO), are explained as crystal disorder of oxygen or zinc [16-18]. Thus, the Raman spectrum and XRD analysis show that the fabricated samples have both the high purity and good crystallyte of ZnO wurtzite structure.

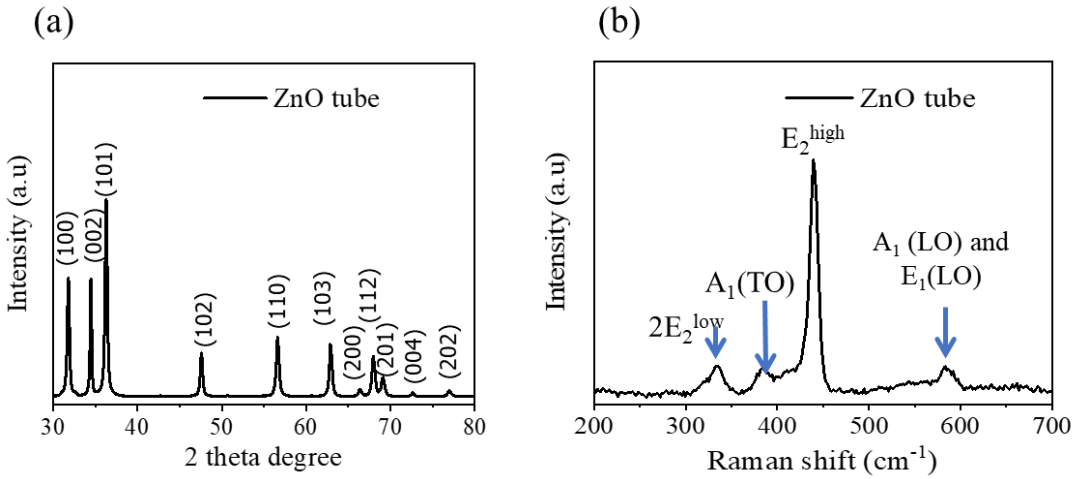

Figure 2. (a) XRD pattern and (b) Raman spectrum of ZnO microtube.

3.2. Study of SERS Mechanism of ZnO Microtube in Detection MB

Firstly, in order to evaluate the SERS activity of the ZnO microtube surface in the detection MB molecule, the normal Raman spectrum of MB was compared to the SERS spectrum of MB at the same concentration of 10^{-4} M. For clearer purpose, the normal Raman and SERS spectra of MB are separated into two windows [400 nm ÷ 1000 nm] and [1000 nm ÷ 1800 nm] and described in Figs. 3a and 3b, respectively. It can be easy to see that most of the tipycal vibaration modes of MB are identical when comparing two of these spectra together. Specifically, the signals show clear observation and separation bands at 449, 501, 597, 672, 770, 1039, 1075 and 1629 cm^{-1}. Among these peaks, the two well-separated bands at 449, 501, and 597 cm^{-1} are attributed to in-plane bending of C-N-C related to the attracted methyl group, and these modes are indicated as totally symmetric vibrations (denoted as A) [13]. The vibration mode center at 672 and is ascribed to in-plane C-C-C vibration associated with fused aromatic ring of MB molecules, and this mode is non-totally symmetric vibration (labled as B) [13]. The 770 band represents mixed vibrations coupled with C-N stretching mode associated with the externally attracted methyl groups of the molecule and in-plane bending C-N-C vibration associated with the fused aromatic ring of the MB molecule; The signature vibration at 951 cm^{-1} is assigned to in-plane C-H bending ascociated with CH_2 rocking modes. These two vibration modes are at 770 and 951 cm^{-1}. This

mode is assigned to totally symmetrical vibration. The band center at 1039 cm^{-1} is attributed to the mixing of in-plane C-H bending and C-S stretching modes, and this mode presents totally symmetric vibrations [13, 19]. The vibration mode at 1075 cm^{-1} is assigned to the contribution of in-plane bending vibrations of both C-H and C-C-C associated with the fused aromatic ring of the MB molecule. This mode is described as a totally symmetric mode. The most intense footprint band at 1625 cm^{-1} is predominantly contributed by stretching (C-C)/(C-N) associated with the fused aromatic ring.

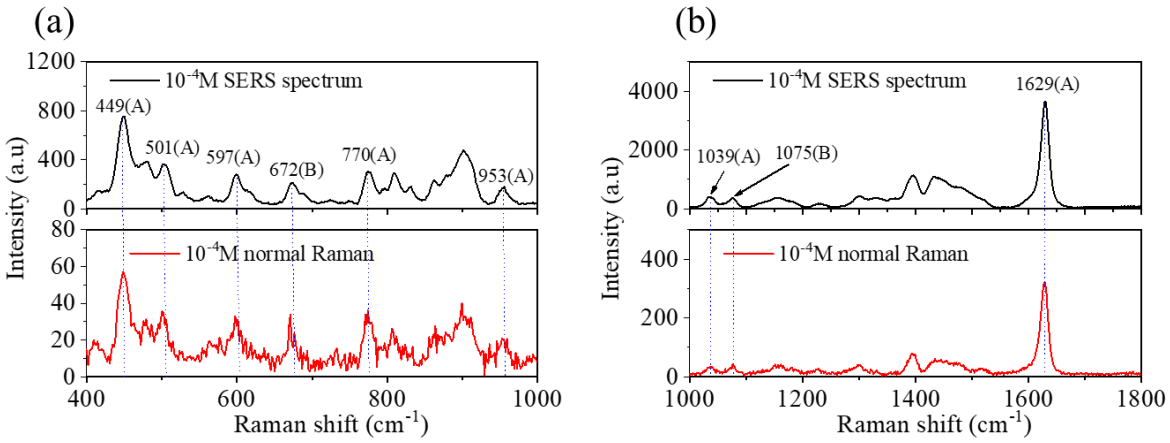

Figure 3. SERS spectra of MB (10^{-4} M) adsorbed on ZnO microtube (red line) in comparison with normal Raman spectra of MB (10^{-4} M) (green line); excitation wavelength at 532 nm.
The symmetric lines are marked as A, and non-totally symmetric lines are labeled as B.

To get in well-understanding of the SERS mechanism based on ZnO microtube in detection MB molecule, a brief introduction of the significant principle of the SERS mechanism for semiconductor materials will be given. It is well-known that SESR mechanism originated from two main mechanisms: electromagnetic enhancement (EM) effect and chemical enhancement [20]. As mentioned above, semiconductor materials with poor conductivity for fewer free electrons generally result in less surface plasmon resonance effect than those of noble metals. Thus, applying semiconductor materials as SERS surface can be advantageous to study the contribution of chemical mechanisms to theirs SERS activity [21].

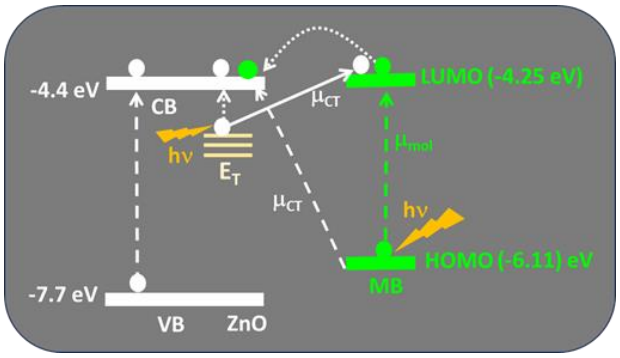

Figure 4. Diagram describing the SERS mechanism based on ZnO microtube substrate in probing MB molecule, under excitation wavelength at 532 nm. Abreviations: HOMO - highest occupied molecular orbital, LUMO - lowest unoccupied molecular orbital, CB – conduction band, VB – valance band, E_T – defect energy, μ_{mol} – molecular resonance, μ_{CT} – charge-transfer resonance.

It should be noted that chemical enhancement is normally composed of three main factors, including: charge-transfer resonance, molecular resonances, and interaction between molecular adsorption and surface without related to resonance phenomena [2, 22]. In this work, for the second possibility, the molecular resonance between MB molecule and ZnO microtube could be neglected due to the laser excitation wavelength (532 nm) being out of resonance with MB molecule [12]. The contribution of interaction between MB molecule and ZnO surface is generally considered a minor contribution to the SERS signal or even ignored in most cases [22, 23]. For the first concern, the charge transfer mechanism played an essential role for the ZnO materials, in which charge transfers from defect states (E_T) of ZnO to LUMO of MB molecule [12]. Figure 4 briefly summarizes the characteristics of the chemical mechanism in SERS activity based on ZnO microtube substrate in detecting MB molecules.

The previous study has been focused on the chemical mechanism with a specific charge transfer mechanism [12]. This work investigates the degree of charge transfer contribution to clarify the role of EM and charge transfer mechanism in SERS activity based on ZnO microtube. According to the Herzberg-Teller selection rules, the only non-totally symmetric state contributing to SERS is the one in which charge-transfer transition occurs. Thus, the degree of charge transfer contribution was calculated using the equation as follows [24, 25]:

$$\rho_{CT}(k) = \frac{I^k(CT) - I^k(SPR)}{I^k(CT) + I^0(SPR)} \quad (3)$$

In which k is an index presenting for individual lines in SERS spectra. $I^k(CT)$ describes the intensity of line k of the SERS spectrum, where it exists the additional contribution of charge transfer to the SERS intensity is due to the SPR effect. In this case, the non-totally symmetric modes (B) of SERS spectra can refer to $I^k(CT)$ and denote as I_{NTSM}; $I^k(SPR)$ corresponds to the intensity of line k, at which only has only the contribution of SPR to the SERS intensity. In general, $I^k(SPR)$ is quite small in the case of non-totally symmetric modes. Therefore, for the sake of simplicity, it could be taken as zero. The last factor is $I^0(SPR)$ presents the intensity of k line which only contributes to the SPR effect and is attributed to the total symmetric line (labeled as I_{TSM}). Therefore, the equation (1) can be rewritten as:

$$\rho_{CT} = \frac{R}{R+1} \quad (4)$$

In which

$$R = \frac{I_{NTSM}}{I_{TSM}} \quad (5)$$

R is the intensity ratio between the non-totally symmetric and totally symmetric SERS spectra. It should be noted that the SERS mechanism is dominated by SPR contribution if ρ approaches 1; If ρ is approximately 0.5 we have the CT and SPR contribution are about equal; and the charge transfer mechanism predominates in the case ρ reaches zero [26].

For the case of the MB molecule, all its specific vibration modes were calculated and clarified in the study of Sannak et al., [13]. To estimate the charge transfer contribution of SERS spectra based on the ZnO microtube, two couple of lines at 597 cm^{-1} (A) + 672 cm^{-1} (B) and 1039 cm^{-1} (B) + 1075 cm^{-1} (A) were chosen thank to they are well-separated and fairly close to each other (Fig. 5). The average value for ρ is approximately 50 (±2)%. Thus, the charge transfer mechanism based on ZnO microtube shows an equal contribution to the SPR mechanism. The high contribution of charge transfer mechanism could result from fairly good SERS activity of ZnO micromicrotube substrate in detection MB compared with the same class semiconductor substrate [7].

This result strengthens the fact that chemical mechanism plays an important role in dielectric materials. In comparison to studies of charge transfer contribution in SERS activity based on other semiconductor materials have been studied such as Cu_2O [27], Ag@Cu_2O core-shell [28], ZnO@Ag

[29], ZnO microtube surface in detection MB molecule shows the more predominant of charge transfer contribution than these ones.

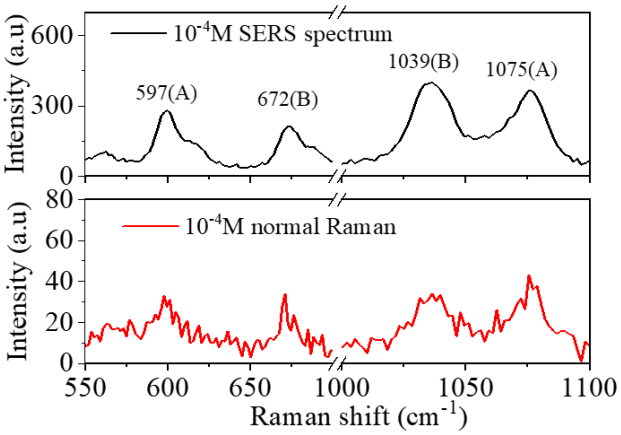

Figure 5. Zoom in on the couple wavenumber regions of symmetric lines and non-totally symmetric lines of the SERS spectrum and normal Raman spectrum of MB.

3.3. Study of SERS Sensitivity Based on ZnO Microtube Surface in Probing MB

To evaluate the sensitivity of SERS activity of ZnO microtube substrate in detecting MB molecule, various concentrations of MB (ranging from 10^{-3} M to 10^{-7} M) were implemented. Figure 6a describes the SERS spectra of MB on ZnO microtube surfaces with the lowest concentration of MB could be recognized at 10^{-7}M. Therefore, the limit of detection (LOD) of MB using ZnO microtube surface is as low as 10^{-7} M. Compared to the previous work also using the same class semiconductor nanomaterial to detect MB[30], the LOD based on ZnO microtube surface is apparently higher than that based on ZnO nanorods. However, when compared to the nanocomposit of ZnO nanorod /Au SERS surface, the ZnO microtube substrate has lower sensitivity in detecting MB [31, 32]. Figure 6b depicts the linear relationship between the logarithm concentration (Log C) and the logarithmic intensity (LogI) of the peak centered at the line of 1626 cm^{-1}. The positive sloping line in the figure suggests that the enhancement of the SERS signal based on ZnO microtube could be attributed to the increase in the number of molecules anchored on the surface.

To quantify the SERS sensitivity of ZnO microtube substrate in probing MB molecule, the enhancement factor (EF) was estimated using the line at 1626 cm^{-1} as follows [33]:

$$EF = \left(\frac{I_{SERS}}{I_{nor}}\right) \times \left(\frac{C_{nor}}{C_{SERS}}\right) \quad (6)$$

In which I_{SERS} and I_{nor} are the SERS intensity and normal Raman spectra of MB on ZnO microtube substrate and glass substrate, respectively. C_{SERS} and C_{nor} correspond to the concentration of MB (10^{-4} M) on ZnO microtube substrate and glass substrate, respectively.

The various SERS substrates based on ZnO microtube covered with various concentrations of MB from 10^{-3} M to 10^{-7} M were prepared and studied to examine the SERS activity of ZnO microtube. The EF values of ZnO microtube SERS surface in detection MB for the ranging concentration from 10^{-4} to 10^{-7} M were calculated from 1.9×10^{3} to 6.1×10^{5}, respectively.

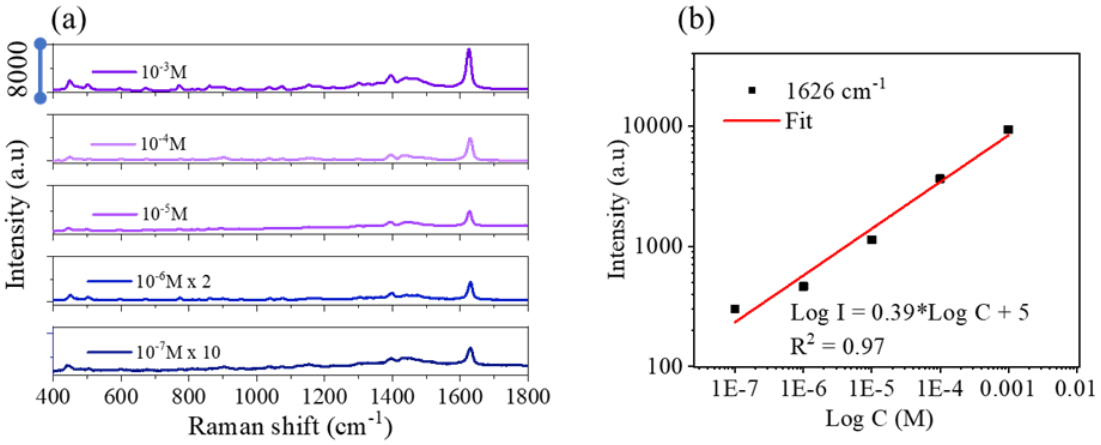

Figure 6. (a) SERS spectra of MB adsorbed on ZnO microtube with different concentrations ranging from 10^{-3} to 10^{-7} M under 532 nm excitation wavelength; and (b) the linear relationship between the log C of MB and the log I of 1626 cm^{-1}.

4. Conclusion

In summary, the SERS substrates based on ZnO microtubes were prepared by hydrothermal growth method and studied SERS activity in probing MB. The SERS mechanism has been evaluated and indicated the equal contribution between SPR and charge transfer mechanism with the charger transfer contribution of 50 (±2) %. The result shows a relatively high contribution of the charge transfer mechanism compared to the SPR mechanism. It could have resulted in the fairly good SERS activity of the ZnO microtube surface with the LOD of 10^{-7} M, and the largest obtained EF is of 6.1×10^5.

Acknowledgments

The author would like to acknowledge the financial support of the Ministry of Education and Training of Vietnam under grand number B2023-TNA-05.

References

[1] [S. Pang, T. Yang, L. He, Review of Surface Enhanced Raman Spectroscopic (SERS) Detection of Synthetic Chemical Pesticides, TrAC Trends in Analytical Chemistry, Vol. 85, 2016, pp. 73-82, https//doi.org/10.1016/j.trac.2016.06.017.

[2] I. Alessandri, J. R. Lombardi, Enhanced Raman Scattering with Dielectrics, Chem Rev, Vol. 116, No. 24, 2016, pp. 14921-14981, https//doi.org/10.1021/acs.chemrev.6b00365.

[3] H. Xu, J. Aizpurua, M. Käll, P. Apell, Electromagnetic Contributions to Single-molecule Sensitivity in Surface-Enhanced Raman Scattering, Physical Review E, Vol. 62, No. 3, 2000, pp. 4318.

[4] B. N. Persson, K. Zhao, Z. Zhang, Chemical Contribution to Surface-Enhanced Raman Scattering, Phys Rev Lett, Vol. 96, No. 20, 2006, pp. 207401, https//doi.org/10.1103/PhysRevLett.96.207401.

[5] R. Pilot, R. Signorini, C. Durante, L. Orian, M. Bhamidipati, L. Fabris, A Review on Surface-Enhanced Raman Scattering, Biosensors (Basel), Vol. 9, No. 2, 2019, https//doi.org/10.3390/bios9020057.

[6] W. Ji, B. Zhao, Y. Ozaki, Semiconductor Materials in Analytical Applications of Surface-enhanced Raman Scattering, Journal of Raman Spectroscopy, Vol. 47, No. 1, 2016, pp. 51-58.

[7] H. D. Aghdam, S. M. Bellah, R. Malekfar, Surface-Enhanced Raman Scattering Studies of Cu/Cu2O Core-Shell NPs Obtained by Laser Ablation, Spectrochim Acta A Mol Biomol Spectrosc, Vol. 223, 2019, pp. 117379, https//doi.org/1016/j.saa.2019.117379.

[8] S. Cong, Y. Yuan, Z. Chen, J. Hou, M. Yang, Y. Su, Y. Zhang, L. Li, Q. Li, F. Geng, Zhao, Noble Metal-Comparable SERS Enhancement from Semiconducting Metal Oxides by Making Oxygen Vacancies, Nat Commun, Vol. 6, 2015, pp. 7800, https//doi.org/10.1038/ncomms8800.

[9] L. G. Quagliano, Observation of Molecules Adsorbed on III-V Semiconductor Quantum Dots by Surface-Enhanced Raman Scattering, Journal of the American Chemical Society, Vol. 126, No. 23, 2004, pp. 7393-7398,

[10] W. Li, R. Zamani, P. R.Gill, B. Pelaz, M. Ibanez, D. Cadavid, A. Shavel, R. A. Puebla, W. J. Parak, J. Arbiol, A. Cabot, CuTe Nanocrystals: Shape and Size Control, Plasmonic Properties, and Use as SERS Probes and Photothermal Agents, Journal of the American Chemical Society, Vol. 135, No. 19, 2013, pp. 7098-7101.

[11] A. Musumeci, D. Gostola, T. Schiler, N. M. Dimitrijevic, V. Mujica, D. Martin, T. Rajh, SERS of Semiconducting Nanoparticles (TiO_2 Hybrid Composites), Journal of the American Chemical Society, Vol. 131, No. 17, 2009, pp. 6040-6041.

[12] T. T. H. Pham, X. H. Vu, T. T. Trang, N. X. Ca, N. D. Dien, P. V. Hai, N.T.H. Lien, N. T. Nghia, N. T. K. Chi, Enhance Raman Scattering for Probe Methylene Blue Molecules Adsorbed on ZnO Microstructures Due to Charge Transfer Processes, Optical Materials, Vol. 120, 2021, https//doi.org/10.1016/j.optmat.2021.111460.

[13] S. D. Roy, M. Ghosh, J. Chowdhury, Adsorptive Parameters and Influence of Hot Geometries on the SER(R) Spectra of Methylene Blue Molecules Adsorbed on Gold Nanocolloidal Particles, Journal of Raman Spectroscopy, Vol. 46, No. 5, 2015, pp. 451-461, https//doi.org/10.1002/jrs.4675.

[14] N. D. Dien, Preparation of Various Morphologies of ZnO Nanostructure through Wet Chemical Methods, Advanced Material Science, Vol. 4, No. 1, 2019, https//doi.org/10.15761/ams.1000147.

[15] L. Zhu, Y. Li, W. Zeng, Hydrothermal Synthesis of Hierarchical Flower-Like ZnO Nanostructure and Its Enhanced Ethanol Gas-Sensing Properties, Applied Surface Science, Vol. 427, 2018, pp. 281-287.

[16] V. Russo, M. Ghidelli, P. Gondoni, C. S. Casari, A. L. Bassi, Multi-Wavelength Raman Scattering of Nanostructured Al-Doped Zinc Oxide, Journal of Applied Physics, Vol. 115, No. 7, 2014, pp. 073508, https//doi.org/10.1063/1.4866322.

[17] R. F. Zhuo, H. T. Feng, Q. Liang, J. Z. Liu, J. T. Chen, D. Yan, J. J. Feng, H. J. Li, S. Cheng, B. S. Geng, X. Y. Xu, J. Wang, Z. G. Wu, P. X. Yan, G. H. Yue, Morphology-Controlled Synthesis, Growth Mechanism, Optical and Microwave Absorption Properties of ZnO Nanocombs, Journal of Physics D: Applied Physics, Vol. 41, No. 18, 2008, pp. 185405, https//doi.org/10.1088/0022-3727/41/18/185405.

[18] A. H. N. Melo, M. A. Macêdo, Permanent Data Storage in ZnO Thin Films by Filamentary Resistive Switching, PLoS One, Vol. 11, No. 12, 2016, pp. e0168515,

[19] C. Li, Y. Huang, K. Lai, B. A. Rasco, Y. Fan, Analysis of Trace Methylene Blue in Fish Muscles Using Ultra-Sensitive Surface-Enhanced Raman Spectroscopy, Food Control, Vol. 65, 2016, pp. 99-105, https//doi.org/10.1016/j.foodcont.2016.01.017.

[20] Z. Mao, W. Song, L. Chen, W. Ji, X. Xue, W. Ruan, Z. Li, H. Mao, S. Ma, J. R. Lombardi, B. Zhao, Metal–Semiconductor Contacts Induce the Charge-Transfer Mechanism of Surface-Enhanced Raman Scattering, The Journal of Physical Chemistry C, Vol. 115, No. 37, 2011,vpp. 18378-18383, https//doi.org/10.1021/jp206455a.

[21] L. Chen, H. Sun, Y. Zhao, Y. Zhang, Y. Wang, Y. Liu, X. Zhang, Y. Jiang, Z. Hua, J. Yang, Plasmonic-Induced SERS Enhancement of Shell-Dependent Ag@Cu2O Core–Shell Nanoparticles, RSC Advances, Vol. 7, No. 27, 2017, pp. 16553-16560, https//doi.org/0.1039/c7ra01187c.

[22] L. Jensen, C. M. Aikens, G. C. Schatz, Electronic Structure Methods for Studying Surface-Enhanced Raman Scattering, Chem Soc Rev, Vol. 37, No. 5, 2008, pp. 1061-1073, https//doi.org/10.1039/b706023h.

[23] K. Kneipp, Chemical Contribution to SERS Enhancement: an Experimental Study on a Series of Polymethine Dyes on Silver Nanoaggregates, The Journal of Physical Chemistry C, Vol. 120, No. 37, 2016, pp. 21076-21081.

[24] J. R. Lombardi, R. L. Birke, A Unified Approach to Surface-Enhanced Raman Spectroscopy, The Journal of Physical Chemistry C, Vol. 112, No. 14, 2008, pp. 5605-5617.

[25] A. P. Richter, J. R. Lombardi, B. Zhao, Size and Wavelength Dependence of the Charge-Transfer Contributions to Surface-Enhanced Raman Spectroscopy in Ag/PATP/ZnO Junctions, The Journal of Physical Chemistry C, Vol. 114, No. 3, 2010, pp. 1610-1614.

[26] J. R. Lombardi, R. L. Birke, A Unified View of Surface-Enhanced Raman Scattering, Accounts of Chemical Research, Vol. 42, No. 6, 2009, pp. 734-742.

[27] T. T. Tran, X. H. Vu, P. T. T. Ha, T. N. Nguyen, D. D. Nguyen, Study of Charge Transfer Contribution to Surface-Enhanced Raman Scattering Activity of Cu\(_2\)O Nano-Octahedral Substrate, Communications in Physics, Vol. 32, No. 4, 2022, https//doi.org/10.15625/0868-3166/16787.

[28] L. Chen, Y. Zhao, Y. Zhang, M. Liu, Y. Wang, X. Qu, Y. Liu, J. Li, X. Liu, J. Yang, Design of Cu 2 O-Au Composite Microstructures for Surface-Enhanced Raman Scattering Study, Colloids and Surfaces A: Physicochemical and Engineering Aspects, Vol. 507, 2016, pp. 96-102, https//doi.org/10.1016/j.colsurfa.2016.07.053.

[29] T. T. Tran, X. H. Vu, T. L. Ngo, T. T. H. Pham, D. D. Nguyen, V. D. Nguyen, Enhanced Raman Scattering Based on a ZnO/Ag Nanostructured Substrate: an In-Depth Study of the SERS Mechanism, Phys Chem Chem Phys, Jun 1, 2023, https//doi.org/10.1039/d2cp05732h.

[30] T. N. Viet, Preparation of ZnO Nanoflowers for Surface Enhance Raman Scattering Applications, VNU Journal of Science: Mathematics - Physics, Vol. 36, No. 1, 2020, https//doi.org/10.25073/2588-1124/vnumap.4369.

[31] V. T. Tran, T. H. Tran, M. P. Le, N. H. Pham, V. T. Nguyen, D. B. Do, X. T. Nguyen, B. N. Q. Trinh, T. T. V. Nguyen, V. T. Pham, M. Q. Luy, A. B. Ngac, Highly Efficient Photo-Induced Surface Enhanced Raman Spectroscopy from ZnO/Au Nanorods, Optical Materials, Vol. 134, 2022, https//doi.org/10.1016/j.optmat.2022.113069.

[32] Q. K. Doan, M. H. Nguyen, C. D. Sai, V. T. Pham, H. H. Mai, N. H. Pham, T. C. Bach, V. T. Nguyen, T. T. Nguyen, K. H. Ho, T. H. Tran, Enhanced Optical Properties of ZnO Nanorods Decorated with Gold Nanoparticles for Self Cleaning Surface Enhanced Raman Applications, Applied Surface Science, Vol. 505, 2020, https//doi.org/10.1016/j.apsusc.2019.144593.

[33] S. Kundu, W. Dai, Y. Chen, L. Ma, Y. Yue, A. M. Sinyukov, H. Liang, Shape-Selective Catalysis and Surface Enhanced Raman Scattering Studies Using Ag Nanocubes, Nanospheres and Aggregated Anisotropic Nanostructures, Journal of Colloid and Interface Science, Vol. 498, 2017, pp. 248-262.